Available online at www.sciencedirect.com
ScienceDirect
Trans. Nonferrous Met. Soc. China 23(2013) 156−160
Transactions of Nonferrous Metals Society of China
www.tnmsc.cn

Welding of shape memory alloy to stainless steel for medical occluder

Shi-xiong LÜ[1], Zhong-lin YANG[2], Hong-gang DONG[2]

1. State Key Laboratory of Advanced Welding and Joining, Harbin Institute of Technology, Harbin 150001, China;
2. School of Materials Science and Engineering, Dalian University of Technology, Dalian 116085, China

Received 18 November 2011; accepted 7 April 2012

Abstract: Dissimilar metal joining between NiTi shape memory alloy (SMA) and stainless steel was conducted. A cluster of NiTi SMA wires were first joined with tungsten inert gas (TIG) welding process, then the NiTi SMA TIG weld was welded to a stainless steel pipe with laser spot welding process. The microstructure of the welds was examined with an optical microscope and the elemental distribution in the welds was measured by electron probe microanalysis (EPMA). The results show that TiC compounds dispersively distribute in the NiTi SMA TIG weld. However, the amount of TiC compounds greatly decreases around the fusion boundary of the laser spot weld between the NiTi SMA and stainless steel. Mutual diffusion between NiTi shape memory alloy and stainless steel happen within a short distance near the fusion boundary, and intermetallic compounds such as Ni_3Ti+(Fe,Ni)Ti appear around the fusion boundary.

Key words: medical occluder; NiTi alloy; shape memory alloy; stainless steel; laser spot welding; dissimilar metal joining; Ni_3Ti; (Fe,Ni)Ti

1 Introduction

Because of the unique shape memory effect [1], super elastic properties [2] and good biocompatibility [3], NiTi shape memory alloy (SMA) is widely used in manufacturing medical equipments in recent years [4]. Stainless steel, as a biocompatible material due to its excellent mechanical properties and corrosion resistance, is still the main material used in the production of medical equipments, for instance, in fixing fractured bones [5]. Medical occluder is an interventional therapy implant and has been extensively applied in clinics, especially for the treatment of congenital heart disease [6,7]. The medical occluder is usually made of NiTi shape memory alloy wires which are welded to stainless steel pipes. Although the welding of NiTi SMA was extensively investigated considering its application prospect in medical equipments [8−10], researches about joining NiTi SMA to stainless steel were still limited at present. LI et al [11] conducted laser brazing of NiTi SMA and stainless steel with Ag-based filler metal. Capacitor discharge welding [12], micro-plasma arc welding [13] and laser welding [14−16] of NiTi SMA to stainless steel wires were investigated. However, further investigation on the dissimilar metal joining of NiTi SMA to stainless steel is necessary to explore the wider application of joint design.

In this work, the joining between a cluster of NiTi SMA wires and a stainless steel pipe for medical occluders will be conducted combining the tungsten inert gas (TIG) welding and laser welding processes. The microstructure of the resultant welds will be examined with an optical microscope and the elemental distribution in the welds will be measured by electron probe microanalysis (EPMA) to illustrate the joining effect.

2 Experimental

The medical occluder was made by joining a cluster of Ni45%−Ti55% SMA wires to 316L stainless steel pipes. The chemical compositions of the 316 L stainless steel pipe in this work are given in Table 1. The dimensions of the stainless steel pipe are shown in Fig. 1. The diameter of a typical NiTi SMA wire is 0.1 mm, and 30 wires consist of a cluster.

Figure 2 reveals the experimental procedure in welding of NiTi SMA wires to a stainless steel pipe. First, the NiTi shape memory alloy wires were worn into a fixture and then melted at one end with a TIG arc (the

Foundation item: Project (50974046/E041607) supported by the National Natural Science Foundation of China
Corresponding author: Hong-gang DONG; Tel: +86-411-84706283; Fax: +86-411-84708389; E-mail: donghg@dlut.edu.cn
DOI: 10.1016/S1003-6326(13)62442-5

Table 1 Chemical compositions of 316L stainless steel (mass fraction, %)

Cr	Ni	Mn	Mo	Fe
17	12	1.5	2.5	Bal.

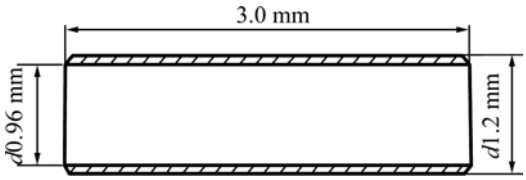

Fig. 1 Dimensions of stainless steel pipe

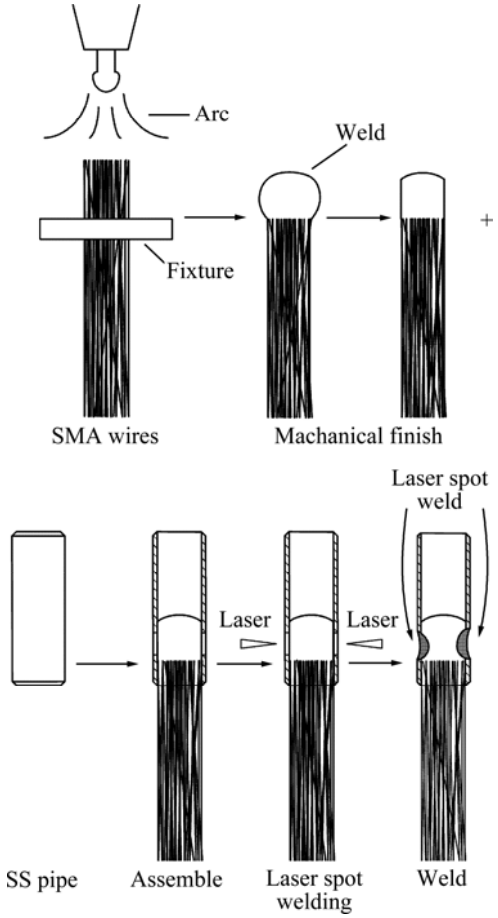

Fig. 2 Experimental procedure during welding of NiTi SMA wires to stainless steel pipe

welding current was 10 A in this experiment). So a ball weld formed at this end of the cluster of NiTi SMA wires. Second, the ball weld was ground with a file until flat, and then the flat TIG weld was put into the stainless steel pipe. Finally, a laser beam spot welding was conducted to join the stainless steel pipe with the TIG weld made from the NiTi SMA wires. The power of the laser beam was 1.1 kW and the laser welding time was 0.5 ms.

The resultant welds between shape memory alloy wires and the stainless steel pipe were cross-sectioned along the radial direction of the pipe and meanwhile across the center of the laser spot weld and followed by a standard metallographic procedure. The specimen was etched with a mixed acid solution (V(HF):V(HNO_3):V(H_2O)=1:2:10)). The microstructure of the weld was examined with an optical microscope, and the elemental distribution in the weld was measured with an electron probe microanalyzer (EPMA−1600) at 15 kV.

3 Results and discussion

Figure 3(a) displays the photo of the resultant medical occluder, which was composed of a cluster of NiTi shape memory alloy wires and 316L stainless steel pipes. And the medical occluder shown in Fig. 3(a) is at working state, that is to say, the shape memory alloy wires are at the memory state. Figure 3(b) shows the laser spot weld between the shape memory alloy wires and the stainless steel pipe.

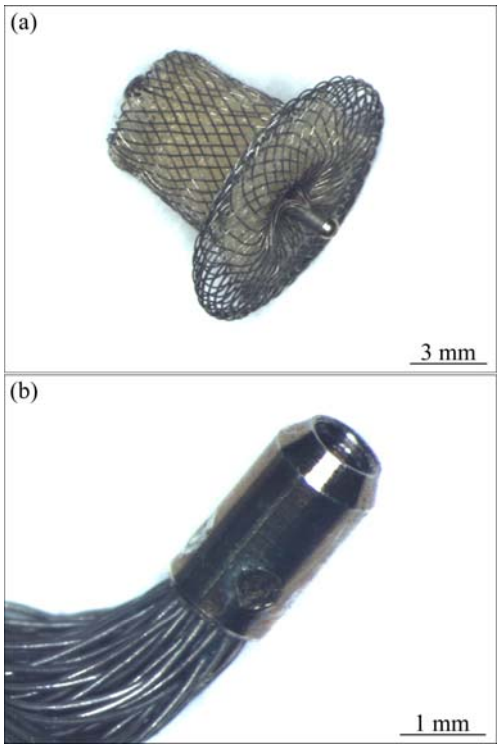

Fig. 3 Photos of medical occluder (a) and laser spot weld between NiTi SMA wires and stainless steel pipe (b)

Figure 4 shows the macrograph and microstructure of the TIG weld and laser spot weld between the NiTi SMA wires and stainless steel pipe. The central part of Fig. 4(a) is the TIG weld of the cluster of NiTi SMA wires, and the laser spot weld between the NiTi SMA wires and the stainless steel located at the top and bottom part of the photo, respectively.

The fusion boundary between the stainless steel and NiTi SMA wires (already melted as TIG weld) can be

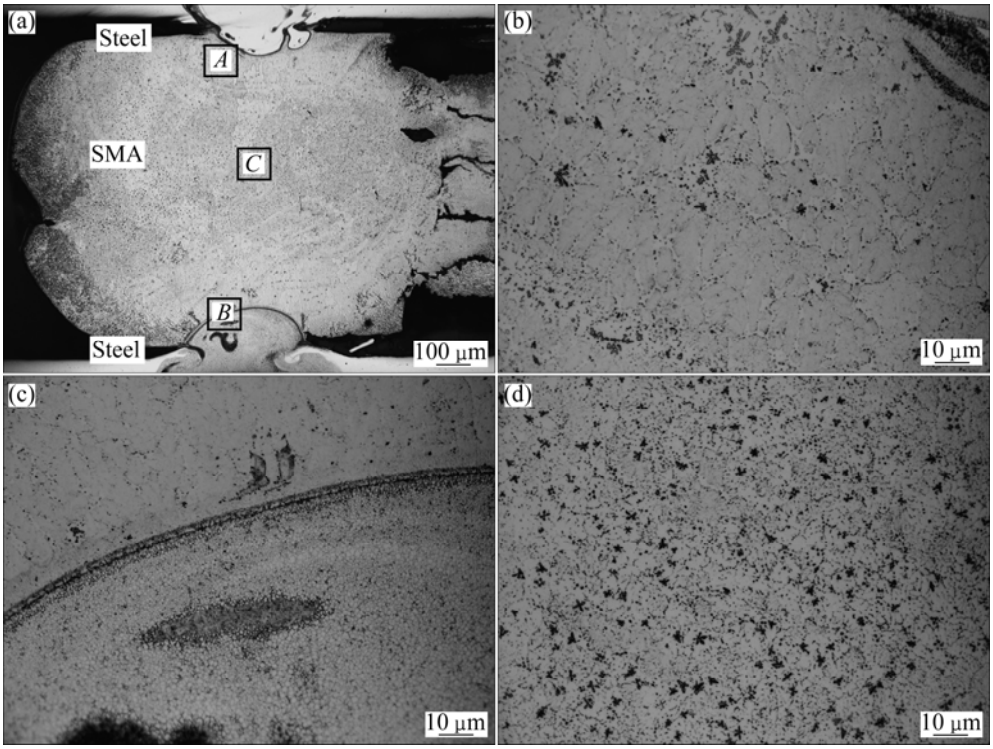

Fig. 4 Microstructures of TIG weld and laser spot weld between stainless steel and NiTi SMA wires: (a) Full view; (b) Area *A*; (c) Area *B*; (d) Area *C*

clearly seen in Fig. 4(a). It can be known from Figs. 4(b) and (c) that the stainless steel joined with the TIG weld. Figure 4(d) displays the microstructure in the center of the NiTi SMA TIG weld, and black asterisk phases dispersively distributed in the matrix, not only in the grain but also along the grain boundary. However, the amount of these black asterisk phases decreased but the grain size coarsened around the fusion boundary, comparing Figs. 4(b) and (d). Since the laser beam directly melted the stainless steel pipe, the heat transferred from the stainless steel welding pool to the NiTi SMA TIG weld which acted as the heat-affected zone during laser spot welding. Although the grains of SMA TIG weld around the fusion boundary coarsened, most of the black asterisk phases disappeared.

To determine the elemental diffusion between the stainless steel pipe and the NiTi SMA TIG weld, EPMA was conducted in the resultant joint. The backscattered electron images and line scanning results are shown in Fig. 5. It can be seen from Fig. 5(d) that Ni and Ti contents have a steep change across the fusion boundary, and a steep change also occurred to Fe and Cr which are the major elements of the stainless steel. The elemental distribution across the fusion boundary confirmed that no mixture happened between the stainless steel and the shape memory alloy in this area around the fusion boundary during the laser spot welding.

Table 2 summarizes the quantitative analysis results at eleven spots in the laser spot weld and NiTi SMA TIG weld, respectively. Spots 1, 2, 3 and 7 locate in the stainless steel side. However, the measurement at Spots 1, 2 and 3 show that the Ti and Ni contents are far higher than the nominal compositions of the stainless steel base metal. Especially, 24%Ti and 40%Ni were detected at Spot 1. However, Ti and Ni contents at Spot 7 are higher but Fe and Cr contents are lower than the nominal compositions of the stainless steel base metal.

Spots 4, 5 and 6 locate around the fusion boundary with Spot 4 close to the stainless steel side and Spot 6 close to the NiTi SMA side. It can be seen from Table 2 that the contents of Ti and Ni increased but the contents of Fe and Cr decreased from Spot 4 to Spot 6 across the fusion boundary. This composition change reflected the diffusion gratitude across the fusion boundary. According to the quantitative analysis results and the Fe−Ni−Ti ternary phase diagram, we can deduce that Spot 6 mainly consisted of Ni−Ti and Fe−Ti intermetallic compounds such as Ni_3Ti+(Fe, Ni)Ti.

Spots 8, 9, 10 and 11 locate in the NiTi shape memory alloy side, so the majority of Ti and Ni were detected in this area. It could be inferred from Table 2 that the black asterisk phase at Spot 9 consisted of TiC and NiTi.

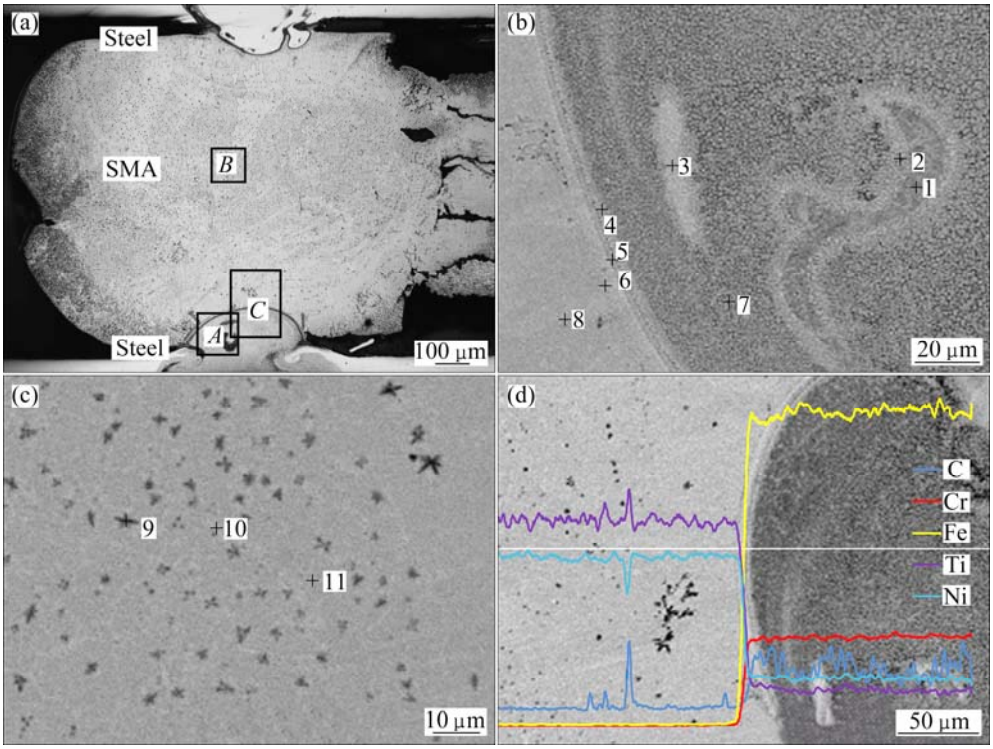

Fig. 5 Backscattered electron images and line scan analysis results in laser spot weld and NiTi SMA TIG weld: (a) Full view; (b) Area *A*; (c) Area *B*; (d) Area *C*

Table 2 EPMA quantitative analysis results in NiTi SMA TIG weld and laser spot weld between TIG weld and stainless steel

Spot No.	*w*(Ti)/%	*w*(Ni)/%	*w*(Fe)/%	*w*(Cr)/%	*w*(C)/%	Possible phase
1	24.014	40.285	24.910	5.158	5.543	
2	16.825	23.529	44.418	11.625	3.602	
3	17.352	28.144	42.906	10.111	1.487	
4	10.678	14.014	57.825	16.083	1.152	
5	25.481	28.429	36.113	8.612	1.365	
6	37.648	55.521	4.942	0.738	1.152	Ni_3Ti+(Fe,Ni)Ti
7	7.824	14.500	60.229	15.417	1.926	
8	42.554	56.315	0.109	0.021	1.001	NiTi
9	53.764	41.946	0.022	0.000	4.269	TiC+NiTi
10	40.029	59.055	0.029	0.000	0.887	NiTi
11	42.349	56.517	0.023	0.000	1.111	NiTi

4 Conclusions

1) While joining a cluster of NiTi shape memory alloy wires to 316L stainless steel pipes, the NiTi shape memory alloy wires can be first TIG welded to form a ball weld and then welded to stainless steel pipes with laser spot welding process.

2) In the laser spot weld, the clear fusion boundary can be seen between the NiTi shape memory alloy and stainless steel, and intermetallic compounds such as Ni_3Ti+(Fe,Ni)Ti appear in fusion boundary. Most of the black asterisk phases of TiC and NiTi in the shape memory alloy TIG weld disappear around the fusion boundary, although the grain size increases during laser spot welding.

References

[1] NAM T H , SABURI T, KAWAMURA Y, SHIMIZU K. Shape memory characteristics associated with the B2→B19 and B19→B19′ transformations in a Ti−40Ni−10Cu (at.%) alloy [J]. Material Transaction, JIM, 1990, 31(4): 262−269.

[2] TORRISI L. The NiTi superelastic alloy application to the dentistry field [J]. Bio-Medical Materials and Engineering, 1999, 99: 39−47.

[3] SHABALOVSKAYA S A. Surface, corrosion and biocompatibility aspects of Nitinol as an implant material [J]. Bio-Medical Materials and Engineering 2002, 12: 69−109.

[4] MORGAN N B. Medical shape memory alloy applications-the market and its products [J]. Materials Science and Engineering A, 2004, 378: 16−23.

[5] DISEGI J A, ESCHBACH L. Stainless steel in bone surgery [J]. Injury, Int J Care Injured, 2000, 31: S-D2−S-D6.

[6] ZHU Y X, XU X D, LIU S Z, LIU J P, CHENG J, FANG J. Domestic occluder interventional therapy for congenital heart disease: A clinical analysis of 20 cases [J]. Anhui Medical and Pharmaceutical Journal, 2010, 14(2): 190−194. (in Chinese)

[7] WANG Z Y, JIN M. Clinical application status of percutaneous interventional closure of ventricular septal defect using amplatzer or homemade occlude [J]. Journal of Cardiovascular & Pulmonary Diseases, 2010, 29(1): 77−80. (in Chinese)

[8] SONG Y G, LI W S, LI L, ZHENG Y F. The influence of laser welding parameters on the microstructure and mechanical property of the as-jointed NiTi alloy wires [J]. Materials Letter, 2008, 62: 2325−2328.

[9] ZHAO X K, WANG W, CHEN L, LIU F J, HUANG J H, ZHANG Hua. Microstructures of cerium added laser weld of a NiTi alloy [J]. Materials Letter, 2008, 61: 115l−1153.

[10] YAN X J, YANG D Z, LIN X P. Corrosion behavior of a laser-welded NiTi shape memory alloy [J]. Materials Characterization, 2007, 58: 623−628.

[11] LI M G, SUN D Q, QIU X M, SUN D X, YIN S Q. Effects of laser brazing parameters on microstructure and properties of TiNi shape memory alloy and stainless steel joint [J]. Materials Science and Engineering A, 2006, 424: 17−22.

[12] LI M G, SUN D Q, QIU X M, SUN D X, YIN S Q. Microstructures and properties of capacitor discharge welded joint of TiNi shape memory alloy and stainless steel [J]. China Welding, 2005, 14(2): 95−100.

[13] QIU X M, SUN D Q, LI M G, LIU W H. Microstructures and properties of welded joint of NiTi shape memory alloy and stainless steel [J]. Transactions of Nonferrous Metals Society of China, 2004, 14(3): 475−479.

[14] LI H M, SUN D Q, HAN Y W, DONG P, LIU C. Microstructures and mechanical properties of laser-welded TiNi shape memory and stainless steel wires [J]. China Welding, 2010, 19(3): 1−5.

[15] GUGEL H, SCHUERMANN A, THEISEN W. Laser welding of NiTi wires [J]. Materials Science and Engineering A, 2008, 481−482: 668−671.

[16] UENISHI K, SEKI M, KUNIMASA T, TAKATSUGU M, KOBAYASHI K F, IKEDA T, TSUBOI A. YAG laser micro welding of stainless steel and shape memory alloy [J]. Proceedings of SPIE, 2003, 4830: 57−62.

医用封堵器中形状记忆合金与不锈钢的焊接

吕世雄[1]，杨仲林[2]，董红刚[2]

1. 哈尔滨工业大学 先进焊接国家重点实验室，哈尔滨 150001；
2. 大连理工大学 材料科学与工程学院，大连 116085

摘　要：研究医用封堵器制造过程中的焊接工艺，首先利用钨极氩弧焊（TIG）将一束 NiTi 形状记忆合金丝焊接在一起，然后采用激光点焊将 NiTi 形状记忆合金丝接头与不锈钢管焊接起来。采用光学显微镜观察接头的显微结构，并利用电子探针（EPMA）研究接头中合金元素的分布。结果表明，在形状记忆合金 TIG 焊接头中弥散分布有 TiC 相，但 TiC 的含量在形状记忆合金与不锈钢的激光点焊焊缝处较少。在熔合线附近存在元素间的相互扩散，并且在熔合线附近产生金属间化合物 Ni_3Ti+(Fe, Ni)Ti。

关键词：医用封堵器；NiTi 合金；形状记忆合金；不锈钢；激光点焊；异种金属连接；Ni_3Ti; (Fe,Ni)Ti

(Edited by Xiang-qun LI)